Zhiwei Huang[1]
Zhihao Wu[1]
Pengcheng Wang[2]
Teng Zhou[1]
Liuyong Shi[1]
Zhenyu Liu[3]
Jiaomei Huang[4]

[1]Mechanical and Electrical Engineering College, Hainan University, Haikou, Hainan, 570228, P. R. China
[2]Department of Mechanical Engineering, University of Houston, Houston, TX, 77204, USA
[3]Changchun Institute of Optics, Fine Mechanics and Physics (CIOMP) 130033, Chinese Academy of Science, Changchun, Jilin, P. R. China
[4]State Key Laboratory of Marine Resource Utilization in South China Sea, Hainan University, Haikou, 570228, P. R. China

Received April 7, 2021
Revised May 24, 2021
Accepted May 26, 2021

Research Article

Multi-particle interaction in AC electric field driven by dielectrophoresis force

When the dielectrophoresis technology is used to manipulate micron-sized particles, the interaction between particles should not be ignored because of the particle-particle interaction. Especially, when multiple particles (number of particles is above 2) are simultaneously manipulated, the interaction between neighboring particles will affect the results of the manipulation. This research investigates the interaction of particles caused dielectrophoresis effect by the Arbitrary Lagrangian-Eulerian (ALE) method based on the hypothesis of the thin layer of the electric double layer at the microscale. The mathematics model can be solved simultaneously by the finite element method for the AC electric field, the flow field around the suspended particles and the particle mechanics at the micrometer scale. In this study, the particle conductivity and the direction of the electric field are investigated, we find that particle conductivity and electric field direction pose an impact on particle movement, and the research reveal the law of microparticle dielectrophoresis movement, which could offer theoretical and technology support to profoundly understand the precise manipulation of particles in microfluidic chips by the dielectrophoresis effect.

Keywords:
Arbitrary Lagrangian–Eulerian (ALE) / Dielectrophoresis / Finite element method / Microfluidics / Multi-particle / Numerical simulation
DOI 10.1002/elps.202100094

1 Introduction

With the development of microdevices, there is an urgent need for a microdevice technology that is easy to operate and highly integrated [1]. According to particle size, shape, density, and electrical properties, the particle manipulation technology can be divided into passive and active method [2–5]. Passive manipulation applies force to the particles by designing corresponding microstructures in the flow channel to achieve particle manipulation, however, passive manipulation has high requirement for chip structure [6,7]. Active manipulation technology refers to the application of the external field to manipulate the particles according to the size characteristics and properties of different types of microparticles. Active manipulation technology includes dielectrophoresis (DEP) [2,8], magnetic field [9–13], acoustic wave [14,15], and optical tweezers [16,17]. Magnetic field method requires magnetic bead marking of target particles. Additionally, acoustic waves method needs the researcher to design a specific microfluidic channel structure to accommodate ultrasonic standing waves. In optical tweezers, lasers used to manipulate particles, simultaneously, long-term manipulation will cause hard-to-recover thermal damage to the particles due to the laser thermal effect. Compared with other methods, the DEP force technology can manipulate particles without damaging them [18]. DEP refers to the phenomenon of particles moving under a spatially non-uniform electric field, regardless of whether the particles are charged or not [8]. The particles are polarized under the action of an external electric field, and the electrical field produces DEP force to drive the particles move. The magnitude of the DEP force is related to the size of the particles and the electrical properties of the particles [3]. Nowadays, the DEP force has become one of the important technologies for micro-nano particles manipulation in microfluidics [19].

In the process of using electric fields to manipulate particles, there will be interactions between particles. If a particle exists in a uniform electric field, it will change the electric field around the particle, causing the non-uniform electric field around another particle. If there are multiple particles, it will affect the electric field around all neighboring particles [20]. The non-uniform electric field makes the two sides of the particle unequally polarized, and produces dielectrophoretic force on the particle surface. The particle–particle interaction force will eventually push the two particles to approach each other because of the DEP force, and eventually form a particle chain parallel to the applied electric field [21, 22], which is the particle assembly technology principle.

Correspondence: Professor Teng Zhou, Hainan University, Mechanical and Electrical Engineering College, Hainan University, Haikou 570228, Hainan, P. R. China
E-mail: zhouteng@hainanu.edu.cn

Abbreviation: **ALE**, Arbitrary Lagrangian–Eulerian; **AC**, alternating current; **DC**, direct current; **DEP**, dielectrophoresis

Color online: See article online to view Figs. 1–9 in color.

Experiments have once shown that, a chain of particles parallel to the applied electric field is eventually formed when two spherical particles are arranged in a straight line at a certain angle with respect to the applied electric field [20,23]. Ai et al. simulates the linear arrangement of particles at a certain angle under a direct current electric field, and studies the effect of particle size on the speed when the particles move together [21]. Mohammad R. Hossan studied the particle shape, size and displacement trajectory of different particles under a DC electric field [22]. The electric fields in the above numerical studies are all DC electric fields. However, AC electric fields are often used in practice [24,25]. In the DC electric field, we have to consider the influence of electrophoresis on the controlled particles [26]. In contrast, in the AC electric field, the effect of electrophoresis on the particles movement can be ignored [8,27]. The particles manipulation in microdevices generally involve multi-particle simultaneous, which should consider the interaction between multi-particles. The interaction between particles and surrounding multi-particles has a great influence on the movement of particles in the micron range. Therefore, it is necessary to study the multiparticle interaction [24,28–30]. Xie studied the movement of particles with different dielectric constants in a DC electric field [31]. Numerical simulation results show that particles with different dielectric constants can move along the direction parallel or perpendicular to the electric field direction. In this manuscript, we study the dielectrophoretic interaction of spherical flexible particles in an AC electric field. Then, we developed a model based on the assumption of thin electric double layer, described by the Arbitrary Lagrangian-Eulerian (ALE) method. Eventually, we obtained the velocity and trajectory of particles with different electrical conductivity and electric field direction by the finite element method. Compared with our previous studies, we consider the conductivity of particles in this study. The mathematical model is more in line with real physical reality, it can accurately reflect the multi-particles movement under the AC electric field and support the design of microparticle manipulation chip as well.

2 Theory

2.1 Mathematical model

In this study, the mathematical model of particle interaction is established under the uniform electric field, as illustrated in Fig. 1. The calculation domain is a square ABCD, and the origin of the two-dimensional coordinate system is established at the center of the square.

In this study, an aqueous solution is selected. The EDL thickness of the charged surface is about 1 nm at 25°C. As the Debye length is only dramatically larger than the dimensional feature length in this study, the EDL assumption is adopted. Also, the net charge inside the electric double layer is zero and we also can ignore the van der Waals force [27]. Additionally, the calculation process is optimized by dimensionless,

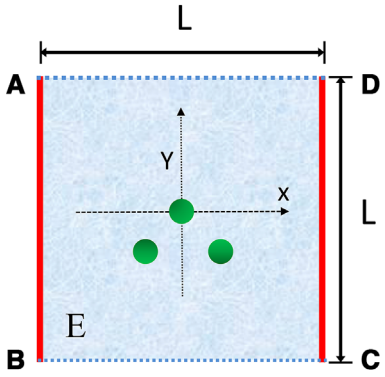

Figure 1. Three particles are suspended in the fluid medium of an AC electric field. The origin of the two-dimensional coordinate system (*x*,*y*) is located at the ABCD geometric center of the square with side length L. The AB and DC sides of the square basin are AC electrodes, and the AD and BC sides are electrically insulated. The direction of the electric field is horizontal. The circles in the figure represent the particles to be studied.

and the superscript symbol "*" represents the dimensionless data. The uniform governing equations are as follows, $U_\infty = (\varepsilon_f {\phi^2}_\infty)/(\eta c)$, particle diameter c, $\phi_\infty = R_0 T/F$, are respectively selected as characteristic velocity U_∞, characteristic length c, where ϕ_∞ is electric potential, R_0 is gas constant, F is the Faraday constant, T is the absolute temperature of water, and $\mathbf{u} = U_\infty \mathbf{u}^*$, $\rho = \eta U_\infty \rho^*/c$, $t = at^*/U_\infty$, $\phi = \phi_\infty \phi^*$. The net charge density is zero in computational domain, and the electric potential is governed Gauss's law, as follows:

$$\nabla^* \cdot (\tilde{\varepsilon}_f^* \nabla^* \tilde{\phi}_f^*) = 0 \tag{1}$$

and

$$\nabla^* \cdot (\tilde{\varepsilon}_p^* \nabla^* \tilde{\phi}_p^*) = 0 \tag{2}$$

The frequency of the AC electric field is 1000 Hz, the electric potential $\tilde{\phi}_1 = 20$ V is applied to the entire section AB, and the electric potential $\tilde{\phi}_2 = -20$ V is applied to the entire section CD. Considering the post-processing specification of the program computation data, we can use the time-average dielectrophoresis force to describe it. In order to ensure the accuracy of the required data, the dielectric constants of the fluid and particles in formulas (1) and (2) are embodied as $\tilde{\varepsilon}_f^* = 1 - j\sigma_f/(\omega\varepsilon_f)$, $\tilde{\varepsilon}_p^* = 1 - j\sigma_p/(\omega\varepsilon_p)$, ε_p and σ_p are the dielectric constant and conductivity of the particles, respectively. ω is the angular frequency of the AC electric field. Here, $j = \sqrt{-1}$ is the imaginary unit. In this study, "~" represents a complex variable.

The electric potential that generates an AC electric field follows:

Apply on the section AB:

$$\tilde{\phi}^* = \frac{\tilde{\phi}_1}{2\phi_\infty} \tag{3}$$

Apply on the section CD:

$$\tilde{\phi}^* = -\frac{\tilde{\phi}_2}{2\phi_\infty} \tag{4}$$

Electrical insulation boundary is applied to the section AD and the section BC:

$$\mathbf{n} \cdot \tilde{\varepsilon}_f^* \nabla^* \tilde{\phi}^* = 0 \tag{5}$$

where **n** is the unit normal vector on the boundary between AD and BC. The normal components of the electric potential and the electric displacement are continuous at the interface between the fluid and the particle, and are expressed by the following equation:

$$\tilde{\phi}_f^* = \tilde{\phi}_p^* \tag{6}$$

$$\mathbf{n} \cdot \tilde{\varepsilon}_f^* \nabla^* \tilde{\phi}^* = \mathbf{n} \cdot \tilde{\varepsilon}_p^* \nabla^* \tilde{\phi}_p^* \tag{7}$$

The flow field is controlled by Navier–Stokes equations. Due to the Reynolds number of the fluid is small, the fluid inertia can be ignored. The governing equation in the flow field follows:

$$\nabla^* \cdot \mathbf{u}^* = 0 \tag{8}$$

$$\mathrm{Re} \frac{\partial \mathbf{u}^*}{\partial t^*} = -\nabla^* p^* + \nabla^{*2} \mathbf{u}^* \tag{9}$$

$$\mathrm{Re} = \rho_f c U_\infty / \eta \tag{10}$$

In the square basin ABCD, the AB and CD sides are symmetrical boundaries, and the AD and BC sides are open boundaries. Also, the flow velocity in the square basin ABCD is zero. The symmetrical boundary is defined as zero normal velocity, and the open boundary is defined as zero normal stress.

In this study, due to the size of numerical model is large, the electroosmotic flow velocity on the wall can be neglected.

The AC electric field does not consider the electrophoresis speed term, and the particle movement speed is only considered by the dielectrophoresis. Therefore, we only consider the time-averaged dielectrophoretic force and hydrodynamic force, which are expressed as follows:

$$\mathbf{F}^*_{DEP} = \int \mathbf{E}^* \cdot \mathbf{n} d\Gamma = \varepsilon_0{}^* \varepsilon_f{}^* \int \left[\mathbf{E}^* \mathbf{E}^* - \frac{1}{2} (\mathbf{E}^* \cdot \mathbf{E}^*) \mathbf{I} \right] \cdot \mathbf{n} d\Gamma \tag{11}$$

$$\mathbf{F}^*{}_{\mathrm{H}} = \int \mathrm{T}_{\mathrm{H}}{}^* \cdot \mathbf{n} d\Gamma = \int \left[-\mathrm{p}^* \mathbf{I} + \eta^* (\nabla \mathbf{u}^*) + (\nabla \mathbf{u}^*)^T \right] \cdot \mathbf{n} d\Gamma \tag{12}$$

$\mathbf{E}^*$ is the externally applied electric field. $\mathbf{E}^* = \nabla^* \tilde{\phi}^*$

The formula equation describing particles motion is:

$$m^*{}_{\mathrm{p}} \frac{\mathrm{d}U^*{}_{\mathrm{p}}}{\mathrm{d}t^*} = \mathbf{F}_{\mathrm{H}}{}^* + \mathbf{F}_{\mathrm{DEF}}{}^* \tag{13}$$

$$x^*{}_{\mathrm{p}} = x^*{}_{\mathrm{p0}} + \int_0^t U^*{}_{\mathrm{p}} dt \tag{14}$$

$$\mathbf{F}_{\mathrm{H}} = \eta U_\infty \mathbf{F}^*{}_{\mathrm{H}} \tag{15}$$

$$\mathbf{T}_{\mathrm{H}} = \eta U_\infty \mathbf{T}^*{}_{\mathrm{H}} / c \tag{16}$$

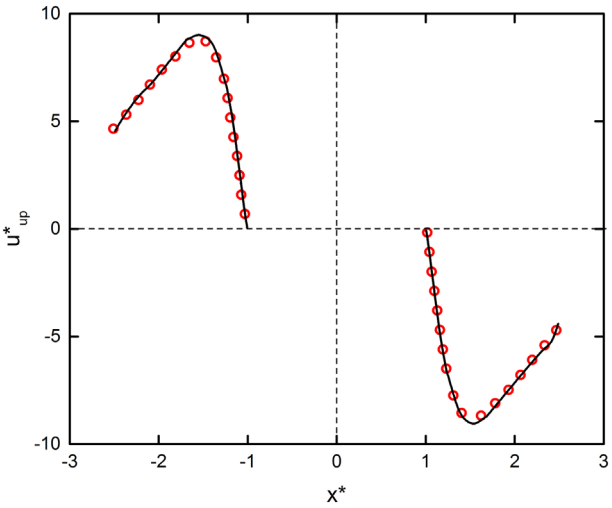

Figure 2. Validation of the model of this study, the relationship between particle *x*-direction displacement and *x*-direction velocity. The solid black line is the result of the Ai et al. research model [27], and the red circle is the result of our research model.

$$\mathrm{m} = \eta c m^*{}_p / U_\infty \tag{17}$$

m_{p} is the mass of the particle, U_{p} is the average speed of the particle, x_{p0} is the initial position of the particle, and x_{p} is the position of the particle at a certain moment.

2.2 Model verification

For code validation, we use this numerical model to simulate the double particles movement under the DEP force in a uniform AC electric field. Ai et al. studied the indeformable circular particles in the AC electric field [27], so under the same parameter conditions, it is consistent with the results of this study. The calculated results are compared with the results of Ai et al., as shown in Fig. 2, the red hollow circle is Ai et al., and the black solid line is the result of this study. It is found that the magnitude of the DEP force on the particles is equal to the model in Ai et al., and the applied DEP force is correct, thus proving the accuracy of the model established in this paper. The simulation results show that the data results overlap, which proves that the developed program can be employed to study the particle DEP motion accurately.

3 Results and discussion

In this paper, we study the influence of several key parameters on the interaction mechanism between the particles, such as the initial position of the particles, the direction of the electric field, and the electrical conductivity. The particle radius is $r =$ 5 μm and the length of the square $L = 500$ μm. In order to simplify the calculation, polystyrene particles are selected as the research object in this study, and the force in the *z*-axis direction of the particles is neglected in the two-dimensional

calculation. The particle density is $\rho_p = 1.0 \times 10^3\ kg/m^3$, the electrical conductivity is $\sigma_p = 4 \times 10^{-4}$ S/m, and the dielectric constant is $\varepsilon_p = 2.6\varepsilon_0$. The conductivity and the dielectric constant of fluid are $\sigma_f = 2 \times 10^{-2}$ S/m, $\varepsilon_f = 80\varepsilon_0$, respectively. The density and viscosity of fluid are divided into $\rho_f = 1.0 \times 10^3$ kg/m^3, $\mu = 1.0 \times 10^{-3}$ kg/(m · s).

Clausius-Mossotti factor $\mathrm{Re}[K(\omega)] = \frac{(\tilde{\varepsilon}_p^* - \tilde{\varepsilon}_f^*)}{(2\tilde{\varepsilon}_f^* + \tilde{\varepsilon}_p^*)}$ can determine whether the particle DEP force is positive or negative, where $\tilde{\varepsilon}_f^* = 1 - j\sigma_f/(\omega\varepsilon_f)$, $\tilde{\varepsilon}_p^* = 1 - j\sigma_p/(\omega\varepsilon_p)$, $\omega = 1000\ \mathrm{Hz} \cdot 2\pi$. The difference in particle conductivity results in different positive and negative Clausius factors, so we can judge whether the DEP force is positive or negative.

When the AC electric field is coupled with the flow field, the particles move by the dielectrophoretic force, and the electrical characteristics of the AC electric field affect the particles movement. In this study, the author obtained the distribution map of the electric field and pressure near the particles in the calculation domain, which can clearly represent the distribution of electric field and pressure around the particles. In order to facilitate the discussion of the DEP interaction and the movement law of the particle in the AC electric field, we analyze and discuss the particle velocity and motion trajectory.

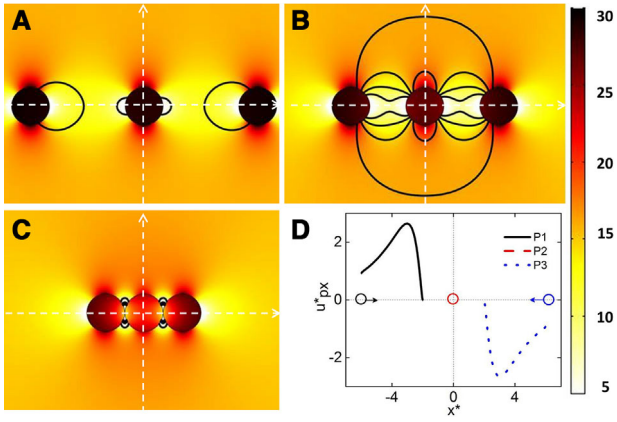

Figure 3. Panels (A–C) are contour diagrams of electric field intensity and flow field pressure near horizontally arranged particles at $t^* = 0$, $t^* = 1.5$ and $t^* = 3$, respectively. Figure 3D shows the relationship between the displacement of the particle in the x direction and the velocity change in the x direction. The hollow circles represent the coordinates of the particle at the initial position. The conductivity of P1, P2, P3 particles is 4×10^{-4} [S/m]. The particle radius is 5 μm. P1, P2, and P3 particle initially locate at (x^*,y^*) = (–6,0), (x^*,y^*) = (0,0), (x^*,y^*) = (6,0), respectively.

3.1 Particles with the same conductivity in the horizontal electric field direction

An electric potential is applied to the AB and CD segments, and the non-uniform electric field is caused by the particles interaction. Additionally, the presence of particles causes distortion of the electric field around the particles, resulting in a non-uniform electric field. Initially, the three particles P1, P2 and P3 are placed in (x^*,y^*) = (–6,0), (x^*,y^*) = (0,0), (x^*,y^*) = (6,0), respectively. The conductivity of P1, P2 and P3 particles are the same $\sigma_p = 4 \times 10^{-4}$ S/m.

Fig. 3A shows the initial position of the particle, and with the application of the electric field, the DEP force acts on the particle, causing the particle to move. According to calculate the Clausius-Mossotti factor, we can get the particles P1, P2, and P3 are $\mathrm{Re}[K(\omega)] < 0$. Therefore, the particles are subjected to negative DEP force, and the negative DEP force will push particles moving toward the direction of low electric field intensity. As Fig. 3B shown, the electric field intensity near the middle particle is low, so the outer particles move closer to the middle particle. Fig. 3C shows the result of particles movement, three particles will cluster into chains eventually. Fig. 3D indicates the relationship between the velocity in the x direction and the displacement in the x direction of the horizontal particles. The hollow black circle represents the initial position of the P1 particle, the hollow red circle represents the initial position of the P2 particle, and the hollow blue circle represents the initial position of the P3 particle. When the AC uniform electric field is acting, the electric field around the particles is distorted due to the existence of the particles, then form a non-uniform electric field and generate DEP force eventually. From Fig. 3D, we can find that the two outer particles move closer to the middle along their horizontal straight line at the same speed. Any one of the three particles will change the uniform distribution of the electric field around the other particles. Therefore, the particles interaction produces the DEP force.

In a non-uniform AC electric field, particles move under the action of the DEP force. As the distance between particles decreases, the DEP force between particles increases and the speed increases. When the P1 particles move closer to the coordinates at (–3,0) and the P2 particles move closer to the coordinates at (3,0), the velocity decreases. From Fig. 3A and B, we can discover that as the particles move closer, the flow field pressure contour becomes denser, and the liquid between the particles is squeezed, which prevents the particles from coming closer together, resulting in a decrease in the movement speed of the particles. Comparing Qian [27] research on the results of the interaction between the particles when the two particles are in the horizontal position, we discover that the two particles and the three particles have the same movement velocity trend, and the particles gain a faster velocity increasing first and then decrease. In this study, it is found that the position of the middle particle does not change when the three particles interact. This result shows that the middle particle plays a positioning role, and helps designing the particles to assemble with each other. Additionally, this result provides theoretical guidance to achieve directional assembly through the two outer particles assemble closer to the middle particle. During the assembly process, the left and right outer particles move closer to the middle particle at the same speed.

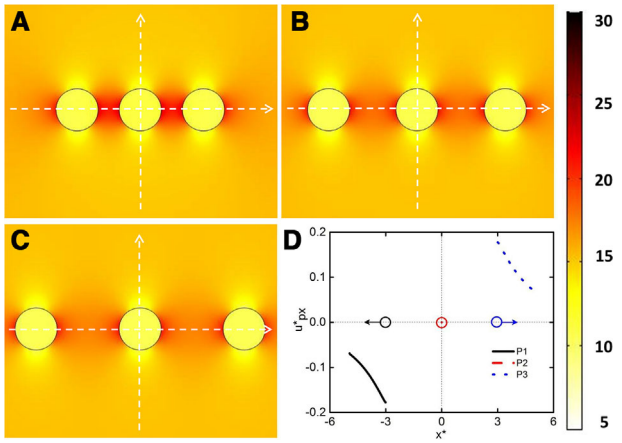

Figure 4. Panels (A–C) are contour plots of electric field intensity and flow field pressure near horizontally arranged particles at $t^* = 0$, $t^* = 9$ and $t^* = 18$, respectively. Panel (D) is the relationship between the displacement of the particle in the x direction and the velocity change in the x direction. The hollow circles represent the coordinates of the particle at the initial position. The conductivity of P1, P2, and P3 particles is 4×10^{-2} [S/m]. The particle radius is 5 μm. P1, P2, and P3 particles initially locate at $(x^*,y^*) = (-3,0)$, $(x^*,y^*) = (0,0)$, $(x^*,y^*) = (3,0)$, respectively.

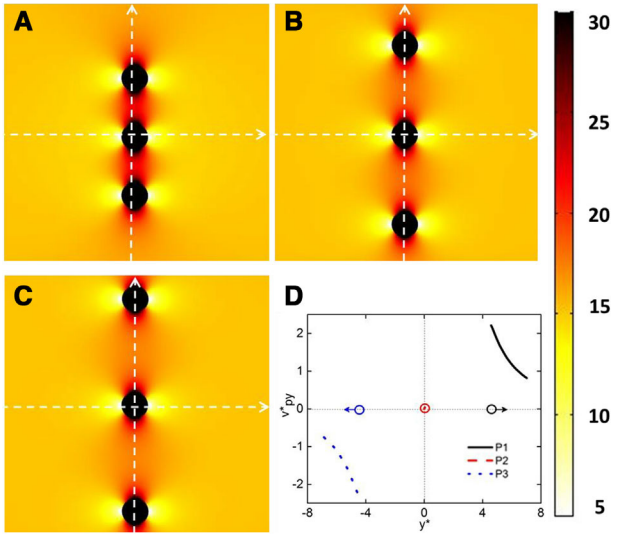

Figure 5. Panels (A–C) are graphs of electric field intensity near vertically arranged particles at $t^* = 0$, $t^* = 2$ and $t^* = 4$, respectively. Panel (D) is a graph of the relationship between the displacement in the y direction of the particle movement and the velocity change in the y direction, and the hollow circles represent the coordinates of the particle at the initial position. The conductivity of P1, P2, and P3 particles is 4×10^{-4} [S/m]. The particle radius is 5 μm, and P1, P2, and P3 particles initially locate at $(x^*,y^*) = (0,4.5)$, $(x^*,y^*) = (0,0)$, $(x^*,y^*) = (0,-4.5)$ respectively.

Considering the different particle conductivity during the assembly process, there will be different positive and negative DEP forces. Below we will discuss the horizontally arranged particles movement when the particle conductivity is 4×10^{-2} [S/m].

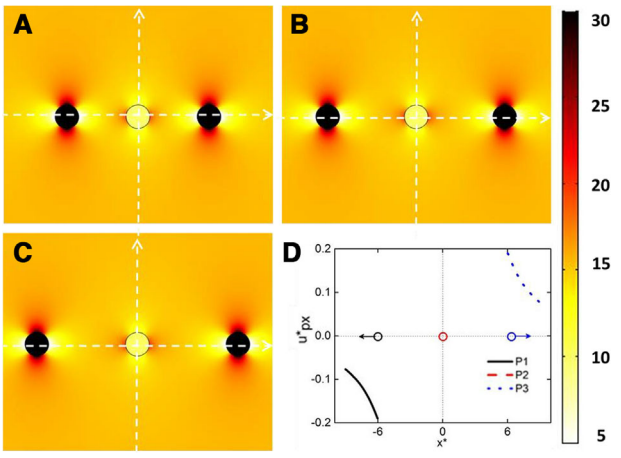

Figure 6. Panels (A–C) are diagrams of electric field intensity near horizontally arranged particles at $t^* = 0$, $t^* = 1.5$ and $t^* = 3$, respectively. Panel (D) shows the relationship between the displacement of the particle and the speed change in the x-direction. The hollow circles represent the coordinates of the particle at the initial position. The conductivity of P1 and P3 particles is 4×10^{-4} [S/m], and the conductivity of P2 particles is 4×10^{-2} [S/m]. The particle radius is 5 μm. P1, P2, and P3 particle initially locate at $(x^*,y^*) = (-6,0)$, $(x^*,y^*) = (0,0)$, $(x^*,y^*) = (6,0)$ respectively.

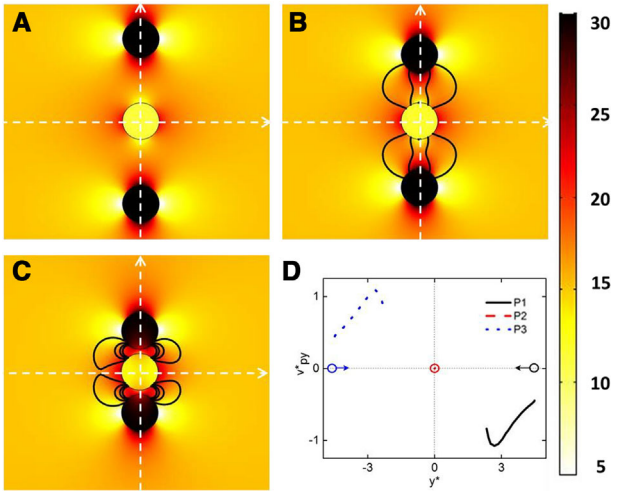

Figure 7. Panels (A–C) are the electric field intensity map and flow field pressure contour map near the vertically arranged particles at $t^* = 0$, $t^* = 1.5$, and $t^* = 3$, respectively. Panel (D) is the relationship between the displacement in the y direction of the particle movement and the velocity change in the y direction. The hollow circles represent the coordinates of the particle at the initial position. The conductivity of P1 and P3 particles is 4×10^{-4} [S/m], and the conductivity of P2 particles is 4×10^{-2} [S/m]. The particle radius is 5 μm, and P1, P2 and P3 particle initially locate at $(x^*,y^*) = (0,4.5)$, $(x^*,y^*) = (0,0)$, $(x^*,y^*) = (0,-4.5)$ respectively.

Through the calculation of Clausius–Mossotti factor, we can obtain the particles will be pushed toward the direction of the strong electric field if particles P1, P2, and P3 are subjected to a positive DEP force. In Fig. 4A, the internal electric field intensity of the three particles is smaller than the external electric field of the particles, and the outer two

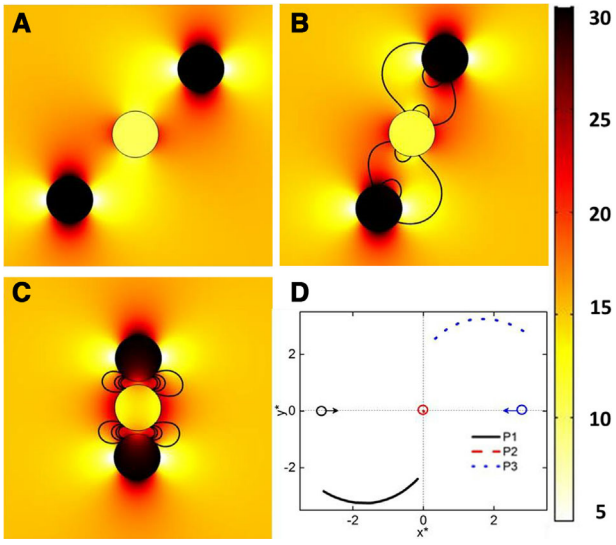

Figure 8. Panels (A–C) are the electric field intensity diagram and flow field pressure contour diagram near 45° linear arrangement of particles at $t^* = 0$, $t^* = 1.5$, and $t^* = 3$, respectively. Panel (D) is the particle trajectory diagram, and the hollow circles represent the coordinates of the particle at the initial position. The conductivity of P1 and P3 particles is 4×10^{-4} [S/m], and the conductivity of P2 particles is 4×10^{-2} [S/m]. The particle radius is 5 μm. P1 particle initially locates at $(x^*,y^*) = (-4.5 \cdot \cos 45°, -4.5 \cdot \sin 45°)$, P2 particle initially locates at $(x^*,y^*) = (0,0)$, P3 particle initially locates at $(x^*, y^*) = (4.5 \cdot \cos 45°, 4.5 \cdot \sin 45°)$.

particles move to the direction of higher electric field intensity as shown in Fig. 4B and C. Fig. 4D shows the relationship between the displacement in the x direction of the particle movement and the velocity change in the x direction, we can discovery that the particle speed reaches the maximum value when the electric field is applied. The electric field distortion is large, resulting in the largest DEP force on the particles. As the distance between the particles becomes longer, the distortion of the nearby electric field by the particles becomes smaller, the particles DEP motion becomes smaller, and the speed becomes smaller. The middle particle is affected by the same effect of the particles on both sides, and it can be found from Fig. 4D that the coordinate of the middle particle does not change in the x direction. This finding shows that not all particles with the same conductivity will move parallel to the electric field lines. Therefore, this finding helps to fully understand the law of microparticle DEP movement.

3.2 Change the direction of the electric field to the same conductivity particles

In the study, we discuss the influence of particle with the same electrical conductivity and the direction of electric field on particle motion. The conductivity of P1, P2, and P3 particles in Fig. 5 is 4×10^{-4} [S/m]. The particle radius is 5 μm. P1 particle initially locates at $(x^*,y^*) = (0,4.5)$, P2 particle initially locates at $(x^*,y^*) = (0,0)$, and P3 initially locates at $(x^*,y^*) = (0,-4.5)$. Through calculating the Clausius–Mossotti factor, we can get the particles P1, P2, and P3 are $\mathrm{Re}[K(\omega)] < 0$. Therefore, the particles are subjected to negative DEP force, and the negative DEP force will push particles moving toward the direction of smaller electric field intensity. In Fig. 5A, it found that the electric field intensity between the particles becomes larger, and the particles move toward the direction of the smaller electric field intensity outside. The force between particles is repulsive force, which can make the distance of the particles farther. When the electric field is applied at the beginning, the particle velocity reaches the maximum value. As the distance between the particles increases, the particles interaction becomes weaker, and the particles velocity decreases until the particles interaction can be ignored. This phenomenon shows that the particles repel each other when the particles are arranged in the vertical direction. In Fig. 1, when the AC electric field electrode is applied to the AB and DC sides, the particles move closer to each other when they are arranged horizontally. Additionally, we can modify the position of the AC electric field electrodes to be on the AD and BC sides, and the particles motion will be changed from close to mutually exclusive. This phenomenon shows that two kinds of particles manipulations can be achieved by changing the position of the AC electric field electrode.

3.3 Interaction of particles with different conductivity

In particle manipulation, it is found that the particles of different property can be manipulated simultaneously. The conductivity of the particles is not necessarily same, so we need to study the mutual movement of particles with different conductivity. In the study of Xie et al., they discuss the particles motion with different dielectric constants under the action of the DC uniform electric field [31]. However, this section discusses the motion of adjacent particles with different conductivity in the AC electric field.

In Fig. 6, the conductivity of P1 and P3 particles is 4×10^{-4} [S/m], and the conductivity of P2 particles is 4×10^{-2} [S/m]. The particle radius of P1, P2, and P3 is 5 μm. P1 particle initially locates at $(x^*,y^*) = (-6,0)$, P2 particle initially locates at $(x^*,y^*) = (0,0)$, P3 particle initially locates at $(x^*,y^*) = (6,0)$. Through the calculation of Clausius–Mossotti factor, we can discovery that P1 and P3 particles are subjected to negative DEP force, and the negative DEP force will push particles moving towards the direction of smaller electric field intensity. The P2 particle is subjected to the positive DEP force, and the positive DEP force will push particles moving towards the direction of stronger electric field intensity. In the Fig. 6A, we can observe that the electric field intensity on the left and right sides of the P1 and P3 particles is smaller than P2 particle, so P1 and P3 particles move away from the P2 particle in the direction of low electric field intensity. As shown in Fig. 6D, the particle velocity values of P1 and P3 reach the

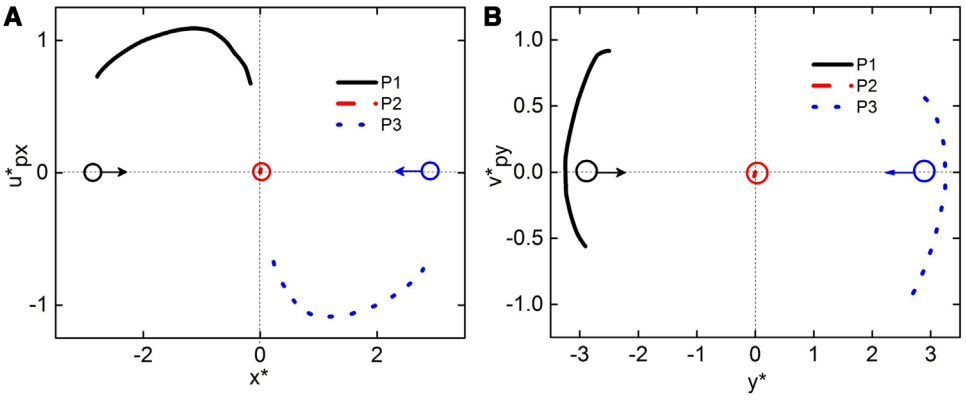

Figure 9. Panels (A) and (B) respectively show the change of the relationship between the particle movement position in the *x* direction and the particle movement velocity in the *x* direction, and the relationship between the particle movement position in the *y* direction and the particle movement velocity in the *y* direction. The hollow circles represent the coordinates of the particle at the starting position.

maximum value when the electric field is applied. As the distance between particles increases, the velocity decreases, due to the particles interaction is becoming weaker. The speed of the middle P2 particles does not change and the position remains unchanged. The phenomenon of mutual repulsion between particles appears, which means that adjacent particles with different conductivity will repel each other when they are arranged in a horizontal straight line. When we want two particles with the same conductivity to repel each other, we can achieve mutual repulsion and separation of particles with the same electrical conductivity by placing particles with different electrical conductivity between them. This phenomenon shows that adding manipulation particles can achieve directional control particle movement.

In Fig. 7, the conductivity of P1 and P3 particles is 4×10^{-4} [S/m], and the conductivity of P2 particles is 4×10^{-2} [S/m]. The particle radius is 5 μm. P1 particle initially locates at $(x^*,y^*) = (0,4.5)$, P2 particle initially locates at $(x^*,y^*) = (0,0)$, and P3 particle initially locates at $(x^*,y^*) = (0,-4.5)$. Through the calculation of Clausius–Mossotti factor, we can know that P1 and P3 particles are subjected to negative DEP force, and the negative DEP force will push particles moving towards the direction of smaller electric field intensity. P2 particle is subjected to a positive DEP force, and the positive DEP force will push particles moving towards the direction of stronger electric field intensity. In Fig. 7A, the electric field intensity on the left and right sides of the P1 and P3 particles is small, and the electric field intensity on the upper and lower sides is large. The upper and lower particles move closer to the place where the middle electric field intensity is small, and the position of the middle particle does not change. This phenomenon is consistent with the movement trend during the horizontal straight arrangement of particles. The particle velocity rapidly increases and then decreases. Compared with Fig. 6, the same conductivity cannot be close in the vertical direction. When the conductivity of the intermediate particles is different, the particles can close together in the vertical direction. Through designing the arrangement of particles with different conductivity, we can arrange the particles to be assembled vertically to achieve the particles of different conductivity close to each other.

In Fig. 8, the conductivity of P1 and P3 particles is 4×10^{-4} [S/m], and the conductivity of P2 particles is 4×10^{-2} [S/m]. The particle radius of P1, P2, and P3 is 5 μm. P1 particle initially locates at $(x^*,y^*) = (-4.5 \cdot \cos 45°, -4.5 \cdot \sin 45°)$, P2 particle initially locates at $(x^*,y^*) = (0,0)$, P3 particle initially locates at $(x^*, y^*) = (4.5 \cdot \cos 45°, 4.5 \cdot \sin 45°)$. Through the calculation of Clausius–Mossotti factor, we can get that P1 and P3 particles are subjected to negative DEP force, and the negative DEP force will push particles moving towards the direction of smaller electric field intensity. P2 particle is subjected to the positive DEP force, and the positive DEP force will push particles moving towards the direction of stronger electric field intensity. In Fig. 8A, the electric field intensity on the left and right sides of the P1 and P3 particles is small, and the upper and lower electric field strengths are large. Fig. 8D shows that P1 and P3 particles repel each other first and then move closer to each other. In Fig. 9, it is found that the displacement and the speed in the *x* direction increase first and then decrease, and the displacement and the speed in the *y* direction decrease from the reverse direction to zero and then increase in the positive direction. As shown in Fig. 8B and C, the flow field pressure contour becomes denser and the resistance between particles increases as the distance between particles decreases. The difference between this study and previous studies [31] is that the variables of this study are particles and solution conductivity, and AC uniform electric field is applied, so the electrophoresis can be ignored.

4 Concluding remarks

Under the micron scale, the particle manipulation is used more extensive in the chemical and biological field, and the requirement for mastering the basic principles of microparticle manipulation is becoming higher. It is necessary to figure out the law of microparticle DEP interaction movement for the design of microfluidic chip. The research results show that the particles parallel to the electric field will approach together by changing the electrical conductivity of the particles, the assembled particles will leave far away each other by changing the direction of the electric field. When the intermediate particles conductivity is different from the

adjacent particles, the particles in the parallel direction of electric field will separate, and the particles in the vertical direction of electric field and 45° inclined to the direction of electric field will be gathered. The results prove that particles interaction movement can be adjusted by the particle conductivity, particle radius and the initial position. Therefore, this study could provide theoretical guidance for particle manipulation, assembly, enrichment, and separation channel design. Additionally, it can help us to understand the principles of DEP technology as well.

This work is funded by National Natural Science Foundation of China (Grant No. 52075138 and No. 61964006) and Hainan Provincial Natural Science Foundation (Grant No. 2019RC032 and No. 519MS021).

The authors have declared no conflict of interest.

Data availability statement

The data that support the findings of this study are available from the corresponding author upon reasonable request.

5 References

[1] Lu, X., Liu, C., Hu, G., Xuan, X., *J. Colloid Interface Sci.* 2017, *500*, 182–201.

[2] Markx, G. H., Carney, L., Littlefair, M., Sebastian, A., Buckle, A.-M., *Biomed. Microdevices* 2009, *11*, 143–150.

[3] Liu, L., Xie, C., Chen, B., Wu, J., *Appl. Math. Mech.* 2015, *36*, 1499–1512.

[4] LaLonde, A., Gencoglu, A., Romero-Creel, M. F., Koppula, K. S., Lapizco-Encinas, B. H., *J. Chromatogr. A* 2014, *1344*, 99–108.

[5] Xuan, X., Zhu, J., Church, C., *Microfluid. Nanofluid.* 2010, *9*, 1–16.

[6] Ai, Y., Joo, S. W., Jiang, Y., Xuan, X., Qian, S., *Electrophoresis* 2009, *30*, 2499–2506.

[7] Patel, S., Showers, D., Vedantam, P., Tzeng, T.-R., Qian, S., Xuan, X., *Biomicrofluidics* 2012, *6*, 034102.

[8] Pethig, R., *Crit. Rev. Biotechnol.* 1996, *16*, 331–348.

[9] Kah, D., Dürrbeck, C., Schneider, W., Fabry, B., Gerum, R. C., *Biophys. J.* 2020, *119*, 15–23.

[10] Yan, J., Skoko, D., Marko, J. F., *Phys. Rev. E: Stat. Nonlinear Soft Matter Phys.* 2004, *70*, 011905.

[11] Chen, Q., Li, D., Zielinski, J., Kozubowski, L., Lin, J., Wang, M., Xuan, X., *Biomicrofluidics* 2017, *11*, 064102.

[12] Liang, L., Zhang, C., Xuan, X., *Appl. Phys. Lett.* 2013, *102*, 234101.

[13] Liang, L., Zhu, J., Xuan, X., *Biomicrofluidics* 2011, *5*, 034110.

[14] Kozuka, T., Yasui, K., Tuziuti, T., Towata, A., Iida, Y., *Jpn. J. Appl. Phys.* 2008, *47*, 4336–4338.

[15] Hwang, J. Y., Cheon, D. Y., Shin, H., Kim, H. B., Lee, J., *Appl. Phys. Lett.* 2015, *106*, 183704.

[16] Bzdek, B. R., Collard, L., Sprittles, J. E., Hudson, A. J., Reid, J. P., *J. Chem. Phys.* 2016, *145*, 054502.

[17] Kim, H., Lee, W., Lee, H.-g., Jo, H., Song, Y., Ahn, J., *Nat. Commun.* 2016, *7*, 13317.

[18] Zhou, T., Deng, Y., Zhao, H., Zhang, X., Shi, L., Woo Joo, S., *J. Fluids Eng.* 2018, *140*, 091302.

[19] Church, C., Zhu, J., Huang, G., Tzeng, T.-R., Xuan, X., *Biomicrofluidics* 2010, *4*, 044101.

[20] Zhou, T., Ji, X., Shi, L., Hu, N., Li, T., *Colloids Surf. A* 2020, *607*, 125493.

[21] Ai, Y., Qian, S., *J. Colloid Interface Sci.* 2010, *346*, 448–454.

[22] Hossan, M. R., Gopmandal, P. P., Dillon, R., Dutta, P., *Colloids Surf. A* 2016, *506*, 127–137.

[23] Zhou, T., Ge, J., Shi, L., Fan, J., Liu, Z., Woo Joo, S., *Electrophoresis* 2018, *39*, 590–596.

[24] Nakajima, Y., Matsuyama, T., *J. Electrostat.* 2002, *55*, 203–221.

[25] Hwang, H., Kim, J.-J., Park, J.-K., *J. Phys. Chem. B* 2008, *112*, 9903–9908.

[26] Hyoung Kang, K., Xuan, X., Kang, Y., Li, D., *J. Appl. Phys.* 2006, *99*, 064702.

[27] Ai, Y., Zeng, Z., Qian, S., *J. Colloid Interface Sci.* 2014, *417*, 72–79.

[28] House, D. L., Luo, H., Chang, S., *J. Colloid Interface Sci.* 2012, *374*, 141–149.

[29] Hossan, M. R., Dillon, R., Dutta, P., *J. Comput. Phys.* 2014, *270*, 640–659.

[30] Hossan, M. R., Dillon, R., Roy, A. K., Dutta, P., *J. Colloid Interface Sci.* 2013, *394*, 619–629.

[31] Xie, C., Chen, B., Ng, C.-O., Zhou, X., Wu, J., *Eur. J. Mech. B Fluids* 2015, *49*, 208–216.

